AMERICAN SOCIETY FOR MICROBIOLOGY | Journal of Virology®

VACCINES AND ANTIVIRAL AGENTS

A Helical Short-Peptide Fusion Inhibitor with Highly Potent Activity against Human Immunodeficiency Virus Type 1 (HIV-1), HIV-2, and Simian Immunodeficiency Virus

Shengwen Xiong,[a,b] Pedro Borrego,[c] Xiaohui Ding,[a,b] Yuanmei Zhu,[a,b] Andreia Martins,[c] Huihui Chong,[a,b] Nuno Taveira,[c,d] Yuxian He[a,b]

MOH Key Laboratory of Systems Biology of Pathogens, Institute of Pathogen Biology, Chinese Academy of Medical Sciences and Peking Union Medical College, Beijing, China[a]; Center for AIDS Research, Chinese Academy of Medical Sciences and Peking Union Medical College, Beijing, China[b]; Research Institute for Medicines, Faculty of Pharmacy, University of Lisbon, Lisbon, Portugal[c]; Centro de Investigação Interdisciplinar Egas Moniz, Instituto Superior de Ciências da Saúde Egas Moniz, Caparica, Portugal[d]

ABSTRACT Human immunodeficiency virus type 2 (HIV-2) has already spread to different regions worldwide, and currently about 1 to 2 million people have been infected, calling for new antiviral agents that are effective on both HIV-1 and HIV-2 isolates. T20 (enfuvirtide), a 36-mer peptide derived from the C-terminal heptad repeat region (CHR) of gp41, is the only clinically approved HIV-1 fusion inhibitor, but it easily induces drug resistance and is not active on HIV-2. In this study, we first demonstrated that the M-T hook structure was also vital to enhancing the binding stability and inhibitory activity of diverse CHR-based peptide inhibitors. We then designed a novel short peptide (23-mer), termed 2P23, by introducing the M-T hook structure, HIV-2 sequences, and salt bridge-forming residues. Promisingly, 2P23 was a highly stable helical peptide with high binding to the surrogate targets derived from HIV-1, HIV-2, and simian immunodeficiency virus (SIV). Consistent with this, 2P23 exhibited potent activity in inhibiting diverse subtypes of HIV-1 isolates, T20-resistant HIV-1 mutants, and a panel of primary HIV-2 isolates, HIV-2 mutants, and SIV isolates. Therefore, we conclude that 2P23 has high potential to be further developed for clinical use, and it is also an ideal tool for exploring the mechanisms of HIV-1/2- and SIV-mediated membrane fusion.

IMPORTANCE The peptide drug T20 is the only approved HIV-1 fusion inhibitor, but it is not active on HIV-2 isolates, which have currently infected 1 to 2 million people and continue to spread worldwide. Recent studies have demonstrated that the M-T hook structure can greatly enhance the binding and antiviral activities of gp41 CHR-derived inhibitors, especially for short peptides that are otherwise inactive. By combining the hook structure, HIV-2 sequence, and salt bridge-based strategies, the short peptide 2P23 has been successfully designed. 2P23 exhibits prominent advantages over many other peptide fusion inhibitors, including its potent and broad activity on HIV-1, HIV-2, and even SIV isolates, its stability as a helical, oligomeric peptide, and its high binding to diverse targets. The small size of 2P23 would benefit its synthesis and significantly reduce production cost. Therefore, 2P23 is an ideal candidate for further development, and it also provides a novel tool for studying HIV-1/2- and SIV-mediated cell fusion.

KEYWORDS HIV-1, HIV-2, fusion inhibitor, short peptide

Received 13 September 2016 **Accepted** 12 October 2016

Accepted manuscript posted online 19 October 2016

Citation Xiong S, Borrego P, Ding X, Zhu Y, Martins A, Chong H, Taveira N, He Y. 2017. A helical short-peptide fusion inhibitor with highly potent activity against human immunodeficiency virus type 1 (HIV-1), HIV-2, and simian immunodeficiency virus. J Virol 91:e01839-16. https://doi.org/10.1128/JVI.01839-16.

Editor Frank Kirchhoff, Ulm University Medical Center

Address correspondence to Yuxian He, yhe@ipb.pumc.edu.cn, or Nuno Taveira, ntaveira@ff.ulisboa.pt.

S.X., P.B., and X.D. contributed equally to this work.

Currently, there are approximately 34 million people worldwide living with human immunodeficiency virus (HIV) (1). Although HIV-1 is a major causative agent of the global AIDS pandemic, about 1 to 2 million people have been infected with HIV-2, mostly in West Africa. In recent decades, HIV-2 also spread to different countries in Europe, Asia, and North America, resulting in the relatively high prevalence of HIV-2 infection. For example, surveillance studies in Portugal and France showed that around 2% of the new infections during 2003 to 2006 were caused by HIV-2 (2, 3), raising additional concerns over the control of AIDS. Therefore, preventive vaccines and therapeutic drugs that are also effective on HIV-2 would be highly appreciated.

HIV-2 was first isolated from AIDS patients in West Africa, and its genome organization was determined from an isolate designated ROD (4, 5). At present, HIV-2 strains are classified in nine groups, termed A to I, of which group A is by far the most disseminated worldwide (ROD is a prototypic HIV-2 group A strain) (6–8). Previous studies demonstrated that HIV-1 and HIV-2 have different evolutionary histories and share only 50% genetic similarity (9, 10). Unfortunately, all currently available antiretroviral drugs were specifically developed to inhibit HIV-1 entry and replication, and consequently some drugs in clinical use have limited or no activity on HIV-2, including all nonnucleoside reverse transcriptase inhibitors, some protease inhibitors, and the fusion inhibitor T20 (enfuvirtide; Fuzeon) (11–14). T20, a 36-mer linear peptide derived from the native gp41 C-terminal heptad repeat (CHR) sequence of the HIV-1 LAI isolate, was approved as the first and, so far, only HIV-1 fusion inhibitor for clinical use (15–17). Mechanically, T20 inhibits HIV-1 entry by competitive binding to the complementary N-terminal heptad repeat (NHR) of gp41, thereby blocking the formation of the six-helical bundle structure (6-HB) that is essential for fusion of the viral and cellular membranes (18–21). Despite its strong anti-HIV-1 activity, T20 easily induces drug resistance through mutations within its NHR-binding sites (22, 23). Also, T20 has poor bioavailability, requiring large-dose injections (90 mg twice daily), which complicates patient adherence to treatment. Furthermore, we and others demonstrated that T20 displayed dramatically decreased activity in inhibiting HIV-2 isolates (14, 24, 25). Considerable efforts have been made to develop new fusion inhibitors with improved pharmaceutical profiles (26–29). T-1249 is a representative second-generation peptide fusion inhibitor that has 39 amino acids derived from the consensus CHR sequences of HIV-1, HIV-2, and simian immunodeficiency virus (SIV); however, its clinical development was hampered beyond phase I/II trials due to the drug formulation difficulties associated with its large size and elevated production costs (30, 31). A number of new inhibitors were designed by using the CHR peptide C34 as a template, and the resulting peptides did show increased anti-HIV-1 activity; however, in most cases they had longer sequences (>34-mer) and still limited activity against HIV-2 isolates (26, 27, 32–34). Finally, some peptides were designed using HIV-2 and/or SIV C34 as templates, generating inhibitors with somewhat improved anti-HIV-2 activity, such as $C34_{EHO}$ and P3 (24, 34).

We recently found that two residues (Met115 and Thr116) preceding the pocket-binding domain (PBD) of CHR peptides adopt a unique M-T hook structure that can greatly enhance the binding and antiviral activities (35–39). Our crystal structures demonstrated that the residue Thr116 can redirect the peptide chain to position Met115 above the left side of the deep pocket on the trimeric coiled coil of N-terminal helices (NHR) so that its side chain caps the pocket to stabilize the inhibitor binding (37–39). On the basis of the M-T hook structure, we generated short-peptide fusion inhibitors that mainly targeted the conserved pocket site of gp41 (37, 40, 41). For example, MTSC22 and HP23 showed dramatically improved inhibition on diverse HIV-1 isolates and high genetic barriers to the development of resistance (37, 41). In this study, we applied the M-T hook strategy to design fusion inhibitors that are also effective on HIV-2 isolates. A 23-mer helical peptide, termed 2P23, was generated that showed very potent inhibitory activities against distinct isolates of HIV-1, HIV-2, and SIV.

TABLE 1 Inhibitory activity of peptide fusion inhibitors on HIV-1 and HIV-2 isolates[a]

Inhibitor	Sequence (no. of aa[b])	Source	IC_{50} (nM)	
			HIV-1_{NL4-3}	HIV-2_{ROD}
Classic peptides				
T20	YTSLIHSLIEESQNQQEKNEQELLELDKWASLWNWF (36)	HIV-1	111.93 ± 3.45	305.55 ± 84.01
C34	WMEWDREINNYTSLIHSLIEESQNQQEKNEQELL (34)	HIV-1	1.02 ± 0.28	387.93 ± 78.32
SFT	SWETWEREIENYTRQIYRILEESQEQQDRNERDLLE (36)	HIV-1	1.1 ± 0.52	105.36 ± 15.08
CP32 M	VEWNEMTWMEWEREIENYTKLIYKILEESQEQ (32)	HIV-1	2.01 ± 0.48	370.95 ± 108.97
SC29	WEEWDKKIEEYTKKIEELIKKSEEQQKKN (29)	HIV-1	1.13 ± 0.84	237.87 ± 74.81
SC22	WEEWDKKIEEYTKKIEELIKKS (22)	HIV-1	54.58 ± 6.94	527.66 ± 80.52
T2635	TTWEAWDR AIAEYAARIEALIRAAQEQQEKNEAALREL (38)	HIV-1	0.38 ± 0.1	18.56 ± 3.21
T1249	WQEWEQKITALLEQAQIQQEKNEYELQKLDKWASLWEWF (39)	HIV-1/HIV-2/SIV	0.97 ± 0.34	10.42 ± 1.96
$C34_{ROD}$	WQEWEKQVRYLEANISKSLEQAQIQQEKNMYELQ (34)	HIV-2	5.51 ± 2.84	48.26 ± 3.7
$C34_{EHO}$	WQQWERQVRFLDANITKLLEEAQIQQEKNMYELQ (34)	HIV-2	1.88 ± 0.35	33.67 ± 4.96
P3	WQEWEQQVRYLEANISQRLEQAQIQQEKNMYELQ (34)	HIV-2/SIV	6.34 ± 1.94	83.23 ± 34.08
M-T hook modified peptides				
MTC34	MTWMEWDREINNYTSLIHSLIEESQNQQEKNEQELL (36)	HIV-1	0.5 ± 0.07	76.61 ± 2.77
MTSFT	MTWETWEREIENYTRQIYRILEESQEQQDRNERDLLE (38)	HIV-1	0.51 ± 0.21	33.93 ± 7.24
MTSC29	MTWEEWDKKIEEYTKKIEELIKKSEEQQKKN (31)	HIV-1	0.43 ± 0.16	22.9 ± 3.9
MTSC22	MTWEEWDKKIEEYTKKIEELIKKS (24)	HIV-1	1.32 ± 0.08	252.24 ± 12.48
$MTC34_{ROD}$	MTWQEWEKQVRYLEANISKSLEQAQIQQEKNMYELQ (36)	HIV-2	0.84 ± 0.29	20.57 ± 2.28
$MTC34_{EHO}$	MTWQQWERQVRFLDANITKLLEEAQIQQEKNMYELQ (36)	HIV-2	1.17 ± 0.16	34.55 ± 2.5
MTP3	MTWQEWEQQVRYLEANISQRLEQAQIQQEKNMYELQ (36)	HIV-2/SIV	1.38 ± 0.32	24.6 ± 2.37
HP23	EMTWEEWEKK IEEYTKKIEEILK (23)	HIV-1	0.19 ± 0.01	78.57 ± 3.02
HP23L	ELTWEEWEKK IEEYTKKIEEILK (23)	HIV-1	0.39 ± 0.06	126.33 ± 9
$P21_{ROD}$	MTWQEWEKQVRYLEANISKSL (21)	HIV-2	571.8 ± 41.3	>1,250
$P21_{EHO}$	MTWQQWERQVRFLDANITKLL (21)	HIV-2	402.35 ± 165.1	>1,250
$P21_{P3}$	MTWQEWEQQVRYLEANISQRL (21)	HIV-2/SIV	534.45 ± 295.78	>1,250
2P23	EMTWEEWEKKVEELEKKIEELLK (23)	HIV-1/HIV-2	0.22 ± 0.05	10.57 ± 0.27
2P23L	ELTWEEWEKK VEELEKKIEELLK (23)	HIV-1/HIV-2	0.59 ± 0.08	18.56 ± 1.31
2P23Q	EMTWQEWEQKVEELEKKIEELLK (23)	HIV-1/HIV-2	1.39 ± 0.45	31.87 ± 7.02

[a]The assay was performed in triplicate and repeated at least 3 times. Data are expressed as means ± standard deviations.
[b]aa, amino acids.

RESULTS

The M-T hook structure can greatly improve the inhibitory activity of diverse inhibitors on HIV-2. To develop a fusion inhibitor that is effective for both HIV-1 and HIV-2, we synthesized and characterized a large panel of CHR peptides (Table 1), including 11 previously reported peptides as controls and 15 newly designed M-T hook-modified peptides as new inhibitors. First, we verified that most of the HIV-1 sequence-derived peptides had markedly decreased activities in inhibiting HIV-2 infection, such as C34, SFT, and SC29. They inhibited NL4-3 replication with 50% inhibitory concentrations (IC_{50}s) of 1.02, 1.1, and 1.13 nM, respectively, but they inhibited ROD with IC_{50}s of 387.93, 105.36, and 237.87 nM, respectively. Even specifically designed HIV-2 sequence-based peptides, such as $C34_{EHO}$ and P3, had much weaker anti-HIV-2 activities than anti-HIV-1 activities. Second, we showed that addition of the M-T hook residues to the N terminus of peptides could dramatically increase their inhibitory potency on both HIV-1 and HIV-2. For example, the M-T hook-modified MTC34, MTSFT, and MTSC29 inhibited NL4-3 with IC_{50}s of 0.5, 0.51, and 0.43 nM, while they inhibited ROD with IC_{50}s of 76.61, 33.93, and 22.9 nM, respectively. Therefore, these results have demonstrated that the M-T hook structure is a vital tool for optimizing an inhibitor against both HIV-1 and HIV-2 isolates.

The M-T hook structure can greatly enhance the binding stability on HIV-2. We previously demonstrated that the M-T hook structure can dramatically enhance the binding affinity of inhibitors to the target by using HIV-1 NHR-derived peptide N36 as a target surrogate (37, 38). To get insights into the mechanism of action, we characterized the interaction between inhibitors and HIV-2 by performing CD spectroscopy. To this end, we synthesized the HIV-2 NHR-derived peptide $N36_{ROD}$ as a target and then compared seven pairs of peptides (C34/MTC34, SFT/MTSFT, SC29/MTSC29, SC22/MTSC22, $C34_{ROD}$/$MTC34_{ROD}$, $C34_{EHO}$/$MTC34_{EHO}$, and P3/MTP3) for their binding stabil-

TABLE 2 Interactions of inhibitors with HIV-1-, HIV-2-, and SIV-derived targets determined by CD spectroscopy[a]

Inhibitor	$N36_{NL4-3}$		$N36_{ROD}$		$N36_{SIV251}$	
	% Helix	T_m (°C)	% Helix	T_m (°C)	% Helix	T_m (°C)
C34	84.5	63.62	30.88	NA	15.61	NA
MTC34	71.95	68.57	50.93	30.76	20.87	NA
SFT	81	69.18	65.64	32.96	25.48	NA
MTSFT	91.68	75.13	102.37	43.76	45.58	39.04
SC29	94.03	65.22	44.4	NA	32.33	NA
MTSC29	98.69	73.98	82.95	46.51	65.13	42.42
SC22	77.01	60.7	43.77	NA	22.09	NA
MTSC22	84.97	71.3	70.05	30.96	71.72	69.93
$C34_{ROD}$	70.87	59.06	50.52	32.91	21.82	NA
$MTC34_{ROD}$	70.22	68.39	100.36	50.4	56.61	45.84
$C34_{EHO}$	70.93	65.83	93.29	45.08	53.12	41.08
$MTC34_{EHO}$	70.18	73.52	107.34	58.24	61.65	53.95
P3	62.79	61.29	61.99	35.41	24.08	NA
MTP3	67.38	69.07	96.72	49.66	45.79	46.01
HP23	86.36	82.18	103.49	43.54	44.99	34.41
$P21_{ROD}$	70.39	48.77	40.51	NA	24.56	NA
$P21_{EHO}$	89.21	55.47	42	NA	18.08	NA
$P21_{P3}$	46.54	NA[b]	32.92	NA	27.61	NA
2P23	102.26	78.79	117.85	55.26	62.51	47.35

[a]The assay was performed 2 times, and results are expressed as means.
[b]NA, not applicable.

ity. Interestingly, all of the M-T hook-modified peptides displayed significantly increased α-helicity compared to their templates (Table 2 and Fig. 1). Thermal denaturation analyses showed that the addition of the M-T hook structure markedly increased the T_m (melting temperature) values of the 6-HB complexes formed between inhibitors and each of HIV-1 and HIV-2 N36 peptides (Table 2 and Fig. 2).

Design of a novel short-peptide inhibitor effective on both HIV-1 and HIV-2. Recently, we demonstrated that a short-peptide fusion inhibitor with potent anti-HIV-1 activity could be developed on the basis of M-T hook structure (37, 40, 41). HP23 and its mutant, HP23L, have only 23 amino acids, but they possess highly potent activity in inhibiting diverse subtypes of HIV-1 isolates and T20-resistant variants. However, our results shown here indicated that both HP23 and HP23L had dramatically reduced activities on HIV-2 ROD, with IC_{50}s of 0.19 versus 78.57 nM and 0.39 versus 126.33 nM, respectively (Table 1). We therefore decided to develop a short-peptide fusion inhibitor that is effective on both HIV-1 and HIV-2 isolates by using the M-T hook strategy and HIV-2 sequence. Disappointingly, three HIV-2-derived short peptides with the M-T hook residues ($P21_{ROD}$, $P21_{EHO}$, and $P21_{P3}$) exhibited poor inhibition on HIV-1 and no inhibition on HIV-2 (Table 1). Encouragingly, a 23-mer peptide, named 2P23, was successfully designed by introducing the critical residues for HIV-2 binding, the salt bridges for peptide stability, and an N-terminal capping residue. First, 2P23 had dramatically improved binding activities on both HIV-1 and HIV-2. As shown in Table 2 and Fig. 3A to D, 2P23 bound HIV-1 N36 and HIV-2 N36 with T_m values of 78.79 and 55.26°C, respectively. Second, 2P23 had largely increased inhibitory activities. As shown in Table 1 and Fig. 3E and F, it inhibited HIV-1 and HIV-2 with IC_{50}s of 0.22 and 10.57 nM, respectively, which were much better than those of HP23. Taken together, these results suggested that 2P23 has promising features as a novel fusion inhibitor peptide.

2P23 efficiently inhibits SIV isolates. We sought to determine whether 2P23 was active against SIV isolates, which are believed to have crossed the species barrier into humans, resulting in HIV-2 and HIV-1. First, we synthesized the SIV NHR-derived peptide $N36_{SIV251}$ as a target and determined its interactions with HP23 and 2P23. As shown in Fig. 4A and B, 2P23 could interact with $N36_{SIV251}$ much more effectively than HP23, with a T_m value of 47.35 versus 34.41°C. We then generated two SIV Env-pseudotyped viruses, SIV_{pbj} and SIV_{239}, and used them in single-cycle infection assays to evaluate the inhibitory activity of 2P23 and three control peptides (T20, P3, and HP23). As shown in

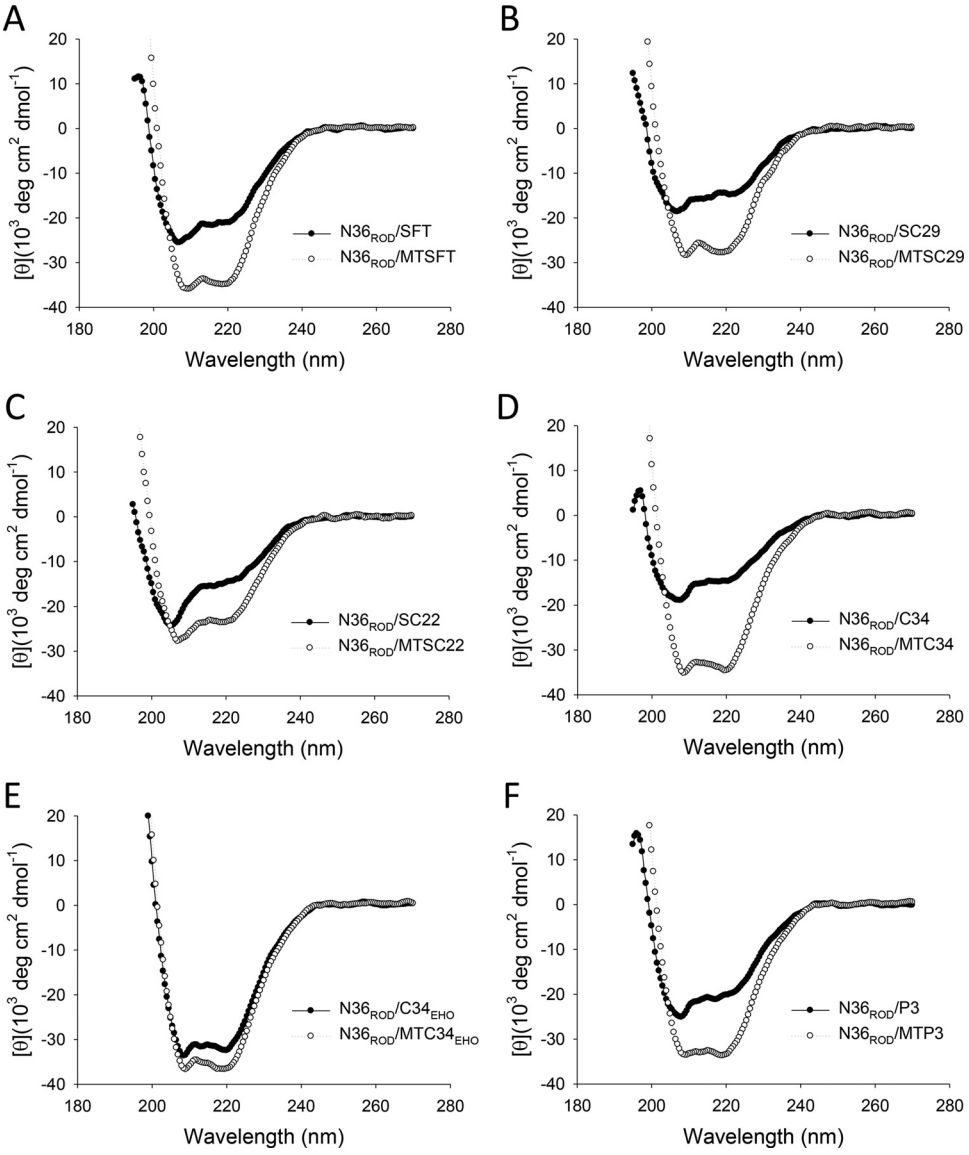

FIG 1 α-Helicity of peptide inhibitors with $N36_{ROD}$ determined by CD spectroscopy. (A) SFT and MTSFT; (B) SC29 and MTSC29; (C) SC22 and MTSC22; (D) $C34_{ROD}$ and $MTC34_{ROD}$; (E) $C34_{EHO}$ and $MT\text{-}C34_{EHO}$; (F) P3 and MTP3. The final concentration of each peptide in PBS was 10 μM.

Fig. 4C and D, 2P23 efficiently inhibited SIV_{pbj} and SIV_{239} with IC_{50}s of 9.96 and 3.34 nM, respectively; in sharp contrast, T20, P3, and HP23 had dramatically decreased activities in inhibiting both SIV isolates. T20, P3, and HP23 inhibited SIV_{pbj} with IC_{50}s of 190.8, 121.8, and 247.7 nM, respectively, and inhibited SIV_{239} with IC_{50}s of 297.67, 17.5, and 105.65 nM, respectively.

2P23 efficiently inhibits HIV- and SIV-mediated cell-cell fusion. We next determined the inhibitory activity of 2P23 and three control peptides (T20, HP23, and P3) on viral Env-mediated cell-cell fusion by a DSP-based assay. In line with its inhibition on viral infection, 2P23 exhibited the most potent activity. As shown in Fig. 5A, 2P23 inhibited $HIV\text{-}1_{NL4\text{-}3}$ Env-mediated cell fusion with a mean IC_{50} of 0.24 nM, whereas T20, P3, and HP23 had mean IC_{50}s of 7.89, 2.25, and 0.33 nM, respectively. Similarly, 2P23 inhibited SIV Env-mediated cell fusion efficiently, with an IC_{50} of 1.8 nM on SIV_{pbj} (Fig. 5B) and an IC_{50} of 2.39 nM on SIV_{239} (Fig. 5C). In sharp contrast, three control peptides had markedly decreased inhibitory activity on SIV Env. T20, P3, and HP23 inhibited SIV_{pbj} at IC_{50}s of 8.35, 3.94, and 7.8 nM, respectively, and they inhibited SIV_{239} with IC_{50}s of 217.33, 6.55, and 17.68 nM, respectively.

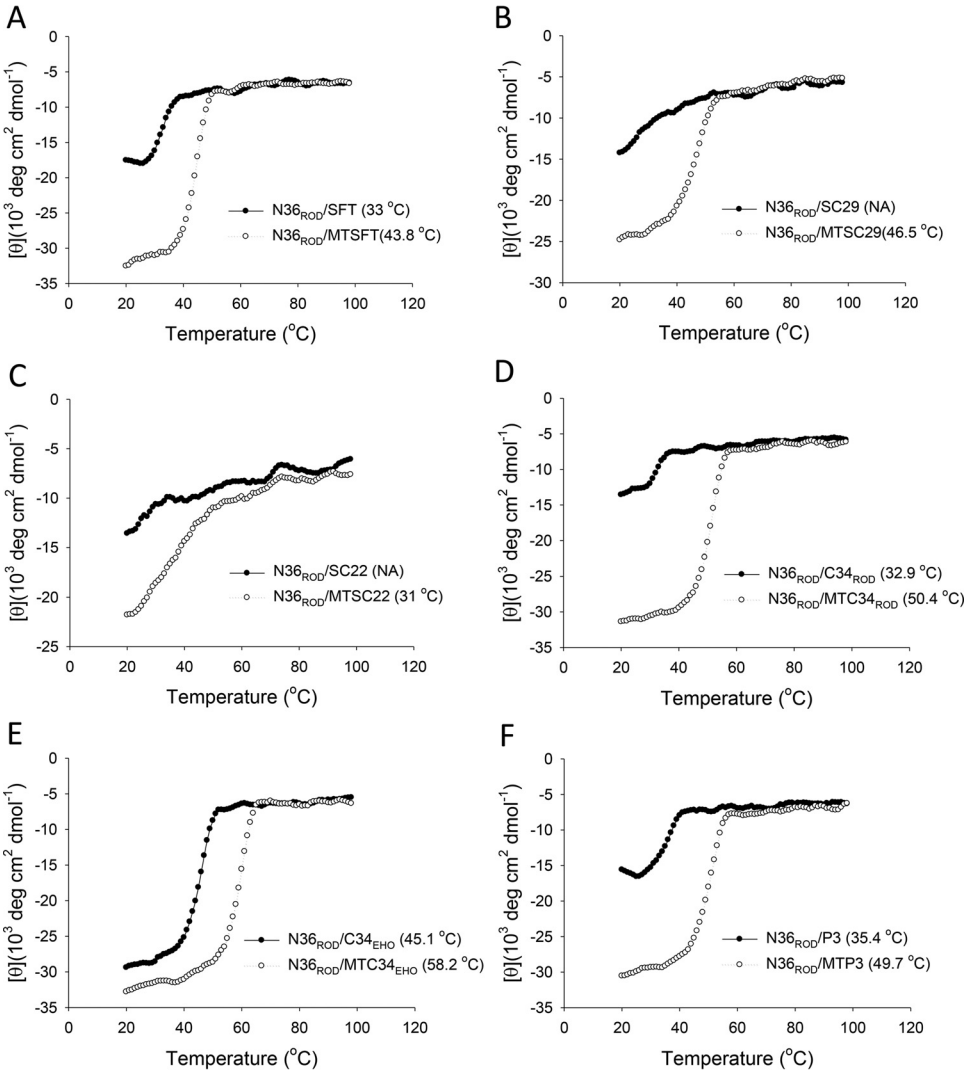

FIG 2 Binding stability of peptide inhibitors with $N36_{ROD}$ determined by CD spectroscopy. (A) SFT and MTSFT; (B) SC29 and MTSC29; (C) SC22 and MTSC22; (D) $C34_{ROD}$ and $MTC34_{ROD}$; (E) $C34_{EHO}$ and MT-$C34_{EHO}$; (F) P3 and MTP3. The final concentration of each peptide in PBS was 10 μM.

2P23 is a potent inhibitor of primary HIV-1 isolates and T20-resistant mutants. As a potential inhibitor for further development, we were intrigued to know whether 2P23 was active, like HP23, on distinct subtypes of HIV-1 isolates and the fusion inhibitor-resistant mutants. Therefore, we assembled a panel of 29 HIV-1 Envs (Table 3), including 3 from subtype A, 6 from subtype B, 3 from subtype B′, 6 from subtype C, 1 from subtype G, 1 from subtype A/C, 4 from subtype A/E, and 5 from subtype B/C. Among them, 12 Env proteins were recently described as a global panel reference that represents the genetic and antigenic diversities of HIV-1 (42). All of the corresponding pseudoviruses were generated, quantified, and used in single-cycle infection assays. As shown in Table 3, 2P23 potently inhibited diverse subtypes of HIV-1 isolates with a mean IC_{50} of 5.57 nM, which was comparable with that of HP23 (4.7 nM). As controls, T20 and P3 inhibited HIV-1 isolates with mean IC_{50}s of 31.49 and 24.35 nM, respectively.

We also constructed a panel of 15 HIV-1_{NL4-3}-based pseudoviruses with Envs carrying T20- or HP23-resistant mutations (43, 44). The inhibition data in Table 4 showed that (i) the long peptides T20 and P3 exhibited relatively higher resistance on T20-resistant mutants, but the short peptides HP23 and 2P23 could maintain their potency, and (ii) 2P23 also displayed improved inhibition over some HP23-resistant mutants (e.g., L57R and L57R/E136G). Taken together, these results indicated that 2P23 is a highly effective

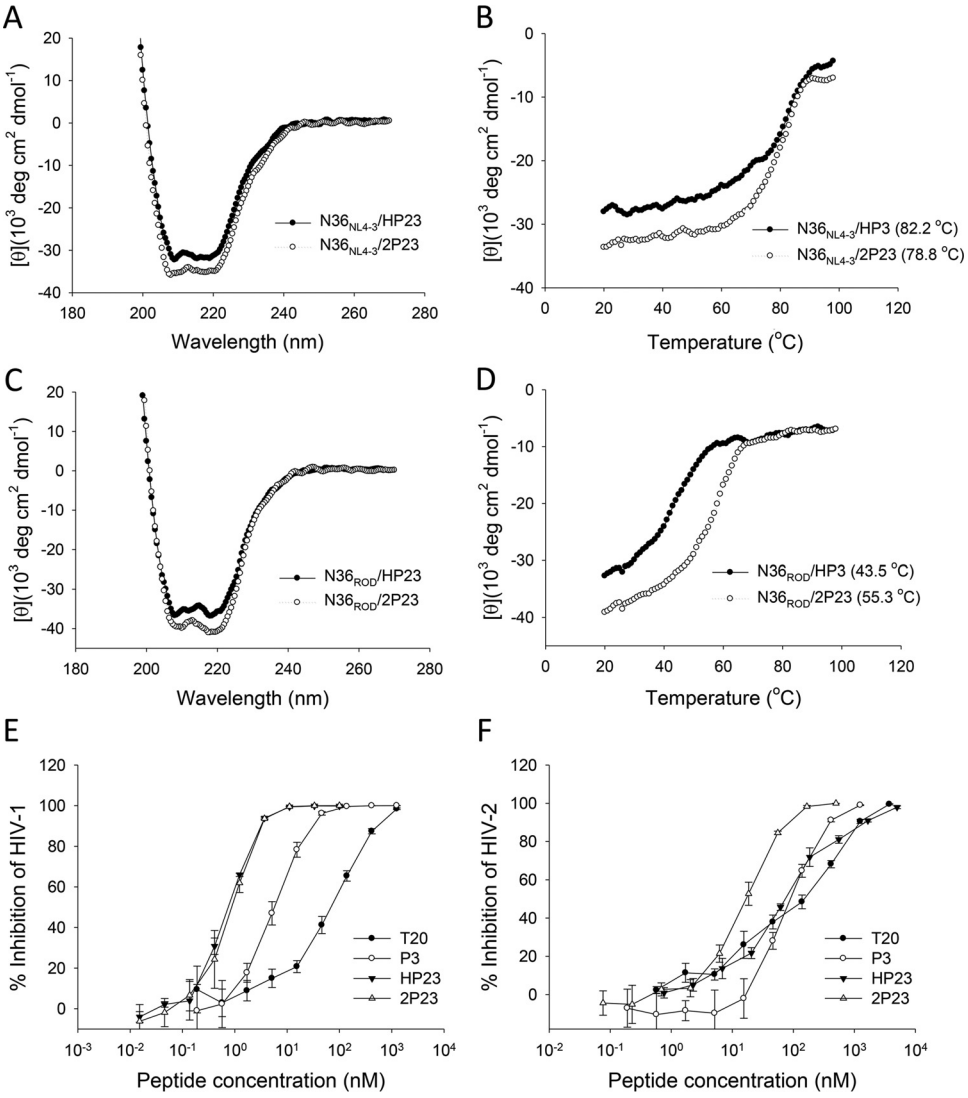

FIG 3 Biophysical properties and anti-HIV activity of 2P23 and control peptides. (A) The α-helicity of HP23 and 2P23 in complexes with $N36_{NL4-3}$. (B) The thermostability of HP23 and 2P23 in complexes with $N36_{NL4-3}$. (C) The α-helicity of HP23 and 2P23 in complexes with $N36_{ROD}$. (D) The thermostability of HP23 and 2P23 in complexes with $N36_{ROD}$. (E) Inhibition of 2P23 and control peptides (T20, P3, and HP23) on infection of $HIV\text{-}1_{NL4-3}$. (F) Inhibition of 2P23 and control peptides (T20, P3, and HP23) on infection of $HIV\text{-}2_{ROD}$. CD experiments were performed with a final concentration of each peptide at 10 μM. The inhibition assays were performed in triplicate and repeated 3 times. Percent inhibition of the peptides and IC_{50}s were calculated as described in the text. Data are expressed as means $\pm$ standard deviations (SD).

fusion inhibitor against diverse subtypes of primary HIV-1 isolates and T20-resistant mutants.

2P23 is a potent fusion inhibitor of diverse primary HIV-2 isolates. One of the main purposes of this study was to create a short-peptide fusion inhibitor that is active for both HIV-1 and HIV-2 isolates. Our above-described data demonstrated that 2P23 had potent activities against a large panel of HIV-1 isolates, one HIV-2 isolate (ROD), and two SIV isolates (SIV_{pbj} and SIV_{239}). In order to demonstrate whether 2P23 had a broad-spectrum anti-HIV-2 activity, we further measured its inhibition on a panel of primary HIV-2 isolates and a panel of ROD-based mutants which utilize different coreceptors (14, 24, 45). Apart from P3 and HP23, the previously reported third-generation peptide inhibitors SFT and T2635 were also included as controls. As shown in Table 5, 2P23 was able to efficiently inhibit infection of distinct primary HIV-2 isolates and ROD mutants, with mean IC_{50}s of 20.17 and 15.38 nM, respectively. T2635 also

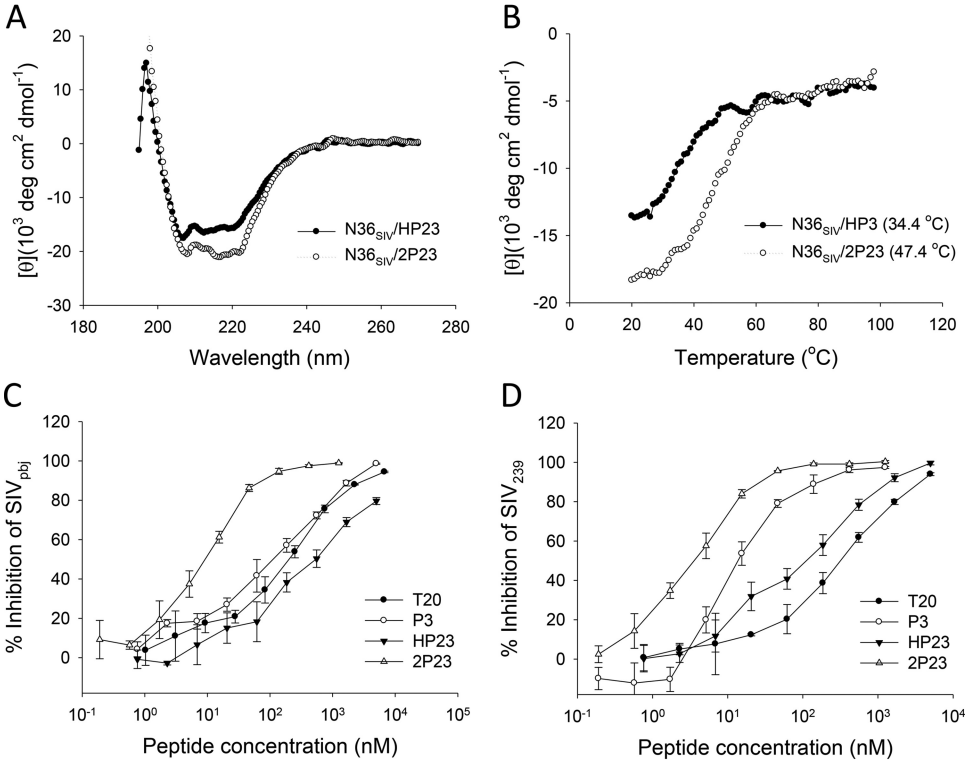

FIG 4 Biophysical properties and anti-SIV activity of 2P23 and control peptides. (A) The α-helicity of HP23 and 2P23 in complexes with $N36_{SIV251}$. (B) The thermostability of HP23 and 2P23 in complexes with $N36_{SIV251}$. (C) Inhibition of 2P23 and control peptides (T20, P3, and HP23) on SIV_{pbj} Env-pseudotyped virus in single-cycle assay. (D) Inhibition of 2P23 and control peptides (T20, P3, and HP23) on SIV_{239} Env-pseudotyped virus in single-cycle assay. CD experiments were performed with a final concentration of each peptide at 10 μM. Single-cycle infection assays were performed in triplicate and repeated 3 times. Percent inhibition of the peptides and IC_{50}s were calculated. Data are expressed as means $\pm$ SD.

exhibited similar inhibitory activity on two panels of viruses, showing mean IC_{50}s of 17.21 and 34.83 nM, respectively. In contrast, SFT, P3, and HP23 showed significantly decreased anti-HIV-2 activity, as they inhibited primary HIV-2 isolates with mean IC_{50}s of 69.96, 64.76, and 62.39 nM, respectively, and inhibited ROD mutants with mean IC_{50}s of 226.12, 191.09, and 94.69 nM, respectively. We conclude therefore that 2P23 is an ideal inhibitor of diverse HIV-2 isolates.

Structural properties of 2P23 in itself. To get more insights into the mechanism underlying the binding and antiviral activities of 2P23 peptide, we determined its own secondary structure and stability by CD spectroscopy. The peptide inhibitors HP23, T20, C34, SFT, T1249, T2635, and P3 were also analyzed for comparison. As shown in Fig. 6A and B, 2P23 alone exhibited high α-helicity at different peptide concentrations, and its thermal unfolding transition (T_m) was dependent on the peptide concentration, which indicated its helical and oligomeric features were similar to those of HP23 (Fig. 6C and D); however, both the helical contents and T_m values of 2P23 at each concentration were much higher than those of HP23. In sharp contrast, T20, C34, and SFT had little or no α-helicity, suggesting their random conformation, while T1249 and P3 displayed much lower levels of helical structures. Although the helical content of the electronically constrained peptide T2635 was comparable to that of 2P23, it had a significantly lower T_m value (40.3 versus 48.1°C), as demonstrated by the data shown in Fig. 6E and F. These results suggest that 2P23 is a helical, oligomeric short-peptide fusion inhibitor having high stability.

DISCUSSION

In the present study, we have dedicated our efforts to developing a short-peptide fusion inhibitor that is effective on both HIV-1 and HIV-2 isolates. First, we verified that

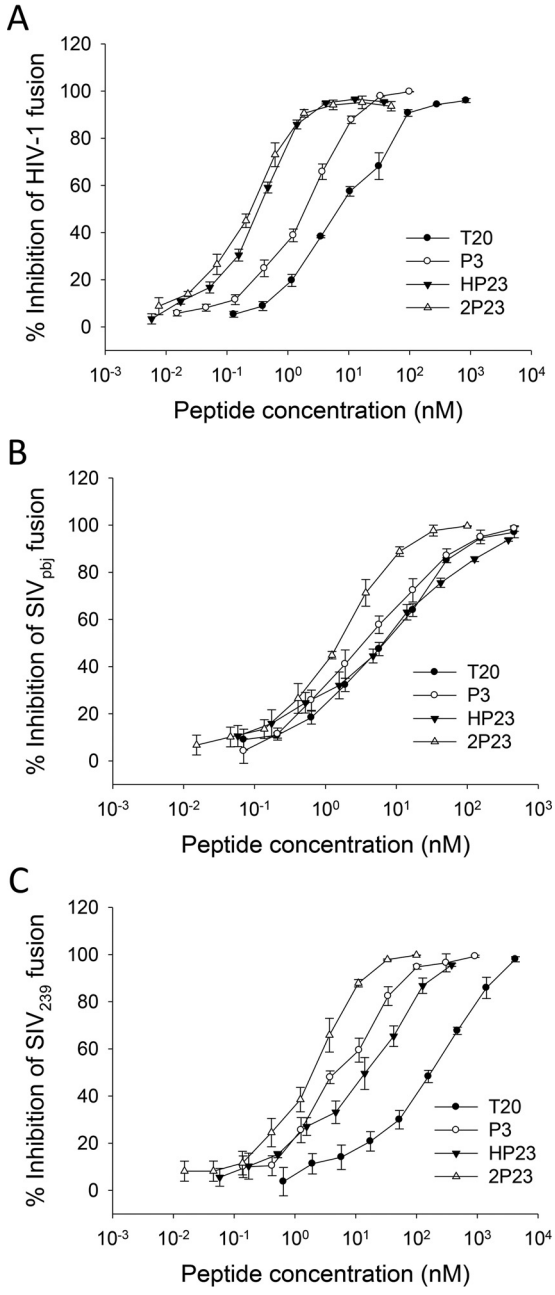

FIG 5 Inhibitory activity of 2P23 and control peptides on Env-mediated cell fusion. Inhibition of 2P23 and control peptides on HIV-1_{NL4-3} Env (A), SIV_{pbj} Env (B), and SIV_{239} Env-mediated cell-cell fusion was measured by DSP-based assays. The experiments were performed in triplicate and repeated at least 2 times. Percent inhibition of the peptides and IC_{50}s were calculated. Data are expressed as means ± SD.

the M-T hook structure strongly boosts the binding and inhibitory activities of CHR-based peptides to the NHR target of HIV-2 isolates, as it does for HIV-1 isolates. We then successfully designed a 23-mer helical peptide, termed 2P23, by adding the M-T hook structure and HIV-2 sequences, which can enhance the inhibitor binding to its target, and introducing the salt bridges that can stabilize the helical structure of the peptide *per se*. Promisingly, 2P23 does show a very potent and broad-spectrum antiviral activity that includes HIV-1, HIV-2, and SIV.

Human (HIV-1/2) and simian (SIV) immunodeficiency viruses infect host cells by fusion of the viral and cellular membranes, which is mediated by viral Env glycoprotein consisting of the surface subunit, gp120, and the transmembrane subunit, gp41.

TABLE 3 Inhibitory activity of 2P23 and control inhibitors on diverse subtypes of HIV-1 isolates[a]

Pseudovirus	Subtype	IC_{50} (nM)			
		T20	P3	HP23	2P23
92RW020	A	10.83 ± 1.65	21.3 ± 3.63	3.28 ± 0.55	2.71 ± 0.92
92UG037.8	A	6.68 ± 1.15	8.56 ± 0.98	2.73 ± 0.26	2.16 ± 0.28
398-F1_F6_20[b]	A	30.48 ± 10.8	24.22 ± 3.4	2.48 ± 0.37	1.6 ± 0.31
SF162	B	7.17 ± 1.3	43.95 ± 1.22	22.10 ± 0.95	15.77 ± 2.48
JRFL	B	49.38 ± 28.4	24.69 ± 2.23	24.51 ± 3.54	8.27 ± 3.24
AC10.0.29	B	3.63 ± 0.38	1.8 ± 0.07	1.13 ± 0.18	1.74 ± 0.54
SC422661.8	B	13.28 ± 1.94	5.88 ± 0.01	1.45 ± 0.06	2.56 ± 0.49
TRO.11[b]	B	18.75 ± 6.37	30.77 ± 7.67	3.68 ± 1.41	5.88 ± 2.37
X2278_C2_B6[b]	B	10.86 ± 1.9	9.85 ± 1.45	2.27 ± 0.4	1.05 ± 0.07
B01	B′	54.48 ± 21.13	68.93 ± 7.19	2.88 ± 0.12	6.35 ± 0.21
B02	B′	42 ± 14.42	83.27 ± 0.04	4.37 ± 1.48	6.56 ± 3.86
B04	B′	12.25 ± 2.52	37.45 ± 18.49	3.09 ± 1.15	6.36 ± 3.02
CAP45.2.00.G3	C	161.36 ± 28.92	87.27 ± 5.19	8.14 ± 4.69	23.59 ± 9.03
ZM109F.PB4	C	12.80 ± 0.76	3.02 ± 0.4	0.91 ± 0.07	1.18 ± 0.21
ZM53 M.PB12	C	35.19 ± 2.13	4.06 ± 0.82	0.91 ± 0.18	1.22 ± 0.43
CE703010217_B6[b]	C	12.36 ± 1.66	8.3 ± 2.98	2.12 ± 0.41	4.52 ± 1.19
CE1176_A3[b]	C	13.56 ± 2.82	22.46 ± 5.54	3.59 ± 0.25	5.20 ± 0.26
HIV_25710-2.43[b]	C	23.38 ± 4.61	5.57 ± 0.44	2.38 ± 0.46	2.53 ± 0.7
X1632-S2-B10[b]	G	12.61 ± 1.77	13.71 ± 0.22	4.25 ± 0.08	4.40 ± 0.99
246_F3_C10_2[b]	A/C	28.59 ± 7.33	11.17 ± 3.15	5.15 ± 1.23	3.12 ± 1.43
AE03	A/E	5.09 ± 2.33	35.38 ± 5.15	1.43 ± 0.54	6.57 ± 0.17
AE04	A/E	9.25 ± 0.62	27.95 ± 6.13	4.33 ± 1.76	8.48 ± 0.67
CNE8[b]	A/E	40.76 ± 18.17	24.76 ± 2.17	4.99 ± 0.08	9.2 ± 1.38
CNE55[b]	A/E	30.82 ± 11.68	18.93 ± 2.04	2.26 ± 0.46	3.25 ± 0.06
CH64.20	B/C	20.15 ± 0.28	2.02 ± 0.32	0.6 ± 0.23	0.61 ± 0.14
CH070.1	B/C	176.6 ± 39.27	26.51 ± 8.71	6.05 ± 0.55	7.83 ± 1.39
CH120.6	B/C	30.25 ± 0.69	29.69 ± 7.2	7.33 ± 0.21	10.19 ± 0.71
CH119.10[b]	B/C	6.21 ± 0.86	13.69 ± 9.07	3.69 ± 0.13	7.33 ± 0.42
BJOX002000.03.2[b]	B/C	34.37 ± 17.2	10.95 ± 3.51	4.06 ± 1.21	1.37 ± 0.57
Mean IC_{50} (range)		31.49 (3.63∼176.6)	24.35 (1.8∼87.27)	4.7 (0.6∼24.51)	5.57 (0.61∼23.59)

[a]The assay was performed in triplicate and repeated at least 3 times. Data are expressed as means ± standard deviations.
[b]A global panel of HIV-1 isolates representing the genetic and antigenic diversities worldwide.

Binding of gp120 to the cellular receptor CD4 and a chemokine coreceptor initiates the fusogenic activity of gp41, resulting in a prehairpin intermediate state in which the fusion peptide of gp41 is inserted into the target membrane. Ultimately, three C-terminal helices (CHR) pack in an antiparallel orientation onto the trimeric coiled coil

TABLE 4 Inhibitory activity of 2P23 and control peptides on drug-resistant HIV-1 mutants[a]

$HIV\text{-}1_{NL4-3}$	T20		P3		HP23		2P23	
	IC_{50} (nM)	*n*-fold	IC_{50} (nM)	*n*-fold	IC_{50} (nM)	*n*-fold	IC_{50} (nM)	*n*-fold
WT	84.09 ± 13.84	1	7.69 ± 0.31	1	0.61 ± 0.13	1	0.69 ± 0.15	1
T20-resistant mutants								
I37T	659.92 ± 79.83	7.85	62.64 ± 0.49	8.15	1.35 ± 0.16	2.21	1.22 ± 0.25	1.77
V38A	1,514.55 ± 246.72	18.01	56.45 ± 10.52	7.34	1.07 ± 0.04	1.75	0.89 ± 0.23	1.29
V38 M	689.42 ± 162.86	8.2	34.03 ± 5.27	4.43	0.99 ± 0.14	1.62	1.21 ± 0.14	1.75
Q40H	2,207.22 ± 519.43	26.25	107.01 ± 21.72	13.92	1.06 ± 0.04	1.74	1 ± 0.27	1.45
N43K	681.7 ± 161.14	8.11	812.6 ± 67.36	105.67	0.79 ± 0.1	1.3	1.13 ± 0.23	1.64
D36S/V38 M	471.88 ± 84.14	5.61	16.67 ± 1.55	2.17	1.39 ± 0.32	2.28	1.48 ± 0.22	2.14
I37T/N43K	6,075 ± 1,572.61	72.24	>2,000	>260.08	1.42 ± 0.13	2.33	1.45 ± 0.32	2.1
V38A/N42T	3,785.94 ± 1,268.36	45.02	86.21 ± 3.43	11.21	0.57 ± 0.13	0.93	0.44 ± 0.1	0.64
HP23-resistant mutants								
E49K	165.4 ± 19.6	1.97	87.38 ± 8.88	11.36	4.45 ± 0.71	7.3	5.2 ± 0.14	7.54
L57R	86.78 ± 4.41	1.03	38.96 ± 1.79	5.07	133.68 ± 5.84	219.15	39.49 ± 0.19	57.23
N126K	182.98 ± 38.03	2.18	12.08 ± 1.28	1.57	1.76 ± 0.04	2.89	1.59 ± 0.77	2.3
E136G	211.4 ± 18.71	2.51	22.72 ± 0.11	2.95	4.73 ± 1.1	7.75	4.66 ± 0.91	6.75
E49K/N126K	203.1 ± 18.48	2.42	134.04 ± 9.33	17.43	5.01 ± 0.45	8.21	4.38 ± 0.8	6.35
L57R/E136G	43.13 ± 14.64	0.51	65.67 ± 2.69	8.54	429.62 ± 93.64	704.3	175.12 ± 46.72	253.8

[a]The assay was performed in triplicate and repeated 3 times. Data are expressed as means ± standard deviations.

TABLE 5 Inhibitory activity of 2P23 and control peptides on diverse HIV-2 isolates[a]

HIV-2 isolate	IC_{50} (nM)				
	SFT	T2635	P3	HP23	2P23
Primary					
00PTHDECT (R5)	30.71 ± 8.86	7.35 ± 3.2	48.89 ± 4.28	99.82 ± 8.29	21.96 ± 5.05
03PTHCC6 (R5)	63.69 ± 0.08	30.11 ± 9.11	114.65 ± 13.45	44.47 ± 14.13	14.51 ± 1.12
03PTHCC19 (R5)	25.7 ± 15.76	43.38 ± 37.01	121.0 ± 11.9	9.14 ± 8.72	7.35 ± 1.57
03PTHCC1 (R5)	16.49 ± 1.47	4.79 ± 1.15	19.36 ± 8.37	2.22 ± 2.08	2.99 ± 0.76
00PTHCC20 (X4)	15.02 ± 13.61	6.79 ± 1.41	13.28 ± 0.65	27.19 ± 5.14	8.74 ± 2
10PTHSMNC (R5)	55.87 ± 2.58	5.33 ± 0.21	86.7 ± 19.3	32.85 ± 8.14	16.4 ± 0.31
03PTHCC12 (R5)	58.85 ± 2.71	16.51 ± 0.12	72.85 ± 19.42	29.3 ± 2.08	24.84 ± 0.53
03PTHSM2 (R5)	98.91 ± 12.99	22.33 ± 0.41	44.02 ± 2.98	98.39 ± 11.22	25.72 ± 2.15
03PTHSM9 (X4)	264.45 ± 32.15	18.29 ± 3.3	62.12 ± 2.07	218.15 ± 37.45	59.04 ± 0.83
Mean IC_{50} (range)	69.96 (15.02∼264.45)	17.21 (4.79∼43.38)	64.76 (13.28∼114.65)	62.39 (2.22∼218.15)	20.17 (2.99∼59.04)
ROD and its mutants					
ROD10 WT (X4)	188 ± 13.5	24.77 ± 14.48	80.59 ± 1.86	57.08 ± 18.31	13.22 ± 2.67
H18L (R5/X4)	312.3 ± 9	49.44 ± 2.54	228.35 ± 8.75	178.8 ± 63.9	16.99 ± 0.56
d23d24 (R5/X4)	174.7 ± 0.3	19.49 ± 0.36	172.65 ± 30.05	82.21 ± 6.35	10.35 ± 0.23
K29T (X4)	179.5 ± 12.7	42.24 ± 0.82	197.15 ± 15.65	52.87 ± 3.88	11.8 ± 1.04
H18L+d23d24 (R5)	274.05 ± 3.35	39.22 ± 1.28	262.3 ± 29.8	113.65 ± 14.66	21.69 ± 1.41
H18L+K29T (R5/X4)	219.55 ± 5.75	24.65 ± 0.52	163.95 ± 1.05	78.41 ± 6.47	15.14 ± 0.47
H18L+d23d24+K29T (R5)	234.75 ± 14.55	44 ± 0.19	232.65 ± 33.35	99.84 ± 5.27	18.46 ± 0.2
Mean IC_{50} (range)	226.12 (174.7∼312.3)	34.83 (19.49∼49.44)	191.09 (80.59∼262.3)	94.69 (52.87∼178.8)	15.38 (10.35∼21.69)

[a]The assays were performed in duplicate and repeated at least 2 times. Data are expressed as means ± standard deviations.

of N-terminal helices (NHR) to form a six-helix bundle (6-HB) structure, which drives the apposition of the viral and cell membranes, resulting in concomitant cell fusion (18, 46, 47). Peptide fusion inhibitors can bind to the exposed NHR or CHR during the prehairpin stage, thereby blocking the formation of 6-HB in a dominant-negative manner (18, 19, 21). However, it was found that the only clinically available HIV-1 fusion inhibitor peptide, T20, and most of the newly developed next-generation peptides had significantly decreased activity in inhibiting HIV-2 isolates (Table 1), thus limiting their potential use for the treatment of HIV-2-infected patients. As noted, the second-generation inhibitor T1249 and the third-generation inhibitor T2635 did exhibit improved potency over HIV-2, but their large sizes (39-mer and 38-mer, respectively) would hamper their formulation and production cost. In an advance stage, the third-generation inhibitor SFT (sifuvirtide) has been approved for clinical phase III trials in China and will hopefully become the next HIV-1 fusion inhibitor in clinical use (33, 35, 48). Nonetheless, our data here indicate that SFT has dramatically decreased inhibitory activity on HIV-2 (Table 1). Additionally, SFT has a similar low genetic barrier to the development of resistance, and the selected HIV-1 variants display high cross-resistance to T20 (35, 49). These data emphasize the importance of developing new fusion inhibitors with significantly improved pharmaceutical profiles.

The structures of both HIV- and SIV-derived 6-HBs revealed the atomic interactions between the NHR and CHR sequences and identified a deep hydrophobic pocket on the NHR helices, which is penetrated by the pocket-binding domain (PBD) of the CHR helix (18, 19, 21, 50–52). Many studies demonstrated that the deep pocket critically determines the NHR-CHR interaction as well as inhibitor binding (18, 19, 21). Our previous studies demonstrated that the M-T hook residues (Met115 and Thr116) preceding the PBD of a CHR peptide can mediate extensive hydrophobic interactions with the pocket, thus dramatically fortifying the binding affinity and antiviral activity of inhibitors (35, 37–39). The results shown here demonstrate that the M-T hook structure also functions well for inhibiting HIV-2 and SIV isolates and suggest that the pocket site is highly conserved among HIV-1/2 and SIV. Importantly, the results also suggest that the M-T hook structure is a general strategy for designing fusion inhibitors with broad-spectrum activity. Obviously, the M-T hook structure is not the only factor for the excellent performance of 2P23. The second design strategy is introducing the residues that are critical for binding HIV-2 NHR, such as valine (V), leucine (L), and glutamic acid (E) (Table

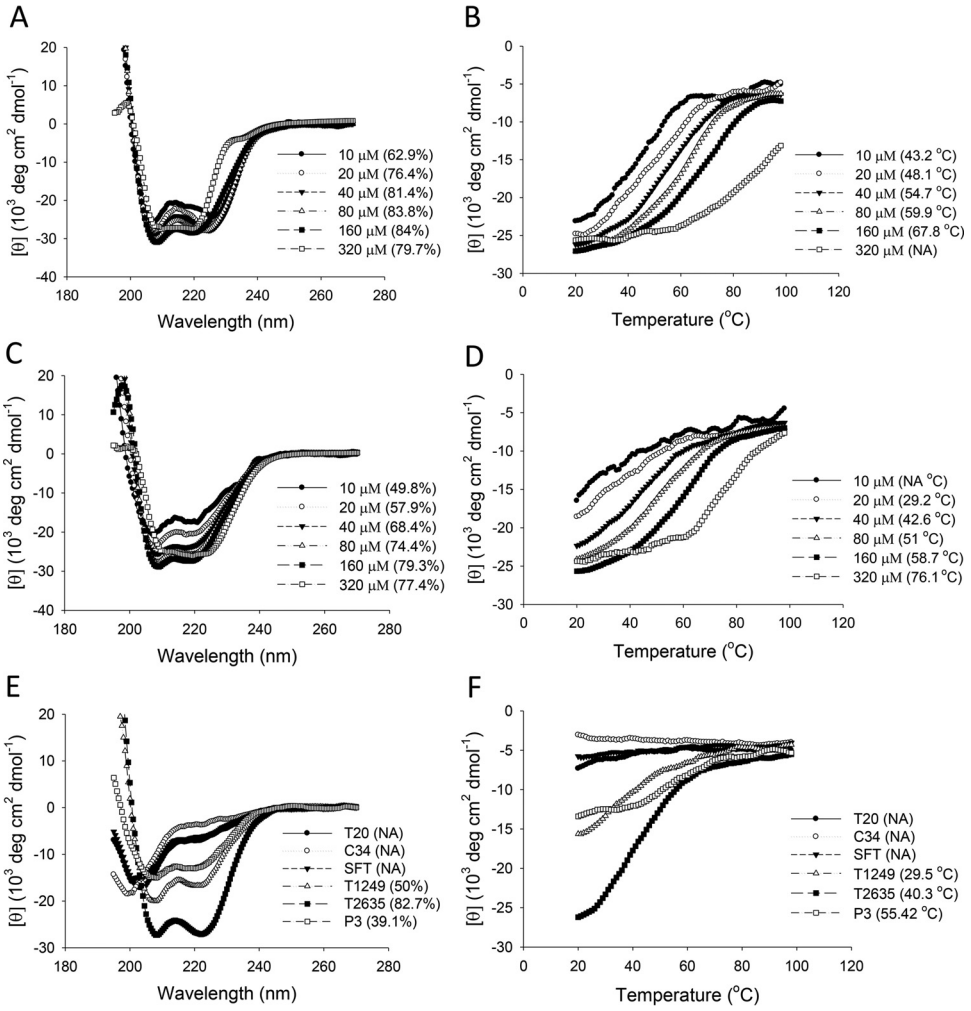

FIG 6 Secondary structure and stability of 2P23 and control peptides determined by CD spectroscopy. The α-helicity (A) and thermostability (B) of 2P23 in itself and the α-helicity (C) and thermostability (D) of HP23 in itself were measured at different concentrations in PBS. The α-helicity (E) and thermostability (F) of control peptides (T20, C34, SFT, T1249, T2635, and P3) were measured at a final concentration of 20 μM in PBS. The helical contents and T_m values are shown in parentheses. NA means not applicable for precise calculation. The experiments were repeated at least two times, and representative data are shown.

1). This is clear when comparing 2P23 and HP23, since both have the M-T hook residues, but 2P23 exhibited greatly improved binding and inhibitory activities to HIV-2 and SIV isolates. The third player for 2P23 is a group of introduced salt bridges, which can facilitate the helical conformation of inhibitor and also stabilize its binding to the NHR target.

In summary, 2P23 has prominent advantages over many other peptide HIV fusion inhibitors. First, it is highly effective on both HIV-1 and HIV-2 isolates. Second, it is only 23 amino acids in length, which will significantly benefit its production. Third, 2P23 binds to the targets with high stability, which can confer a high genetic barrier to resistance. Therefore, we conclude that 2P23 has high potential for clinical development. Also, it provides a novel tool for exploring the mechanisms of HIV and SIV Env-mediated cell fusion.

MATERIALS AND METHODS

Cells and reagents. HEK293T cells were purchased from the American Type Culture Collection (ATCC; Rockville, MD). TZM-bl indicator cells stably expressing large amounts of CD4 and CCR5, along with endogenously expressed CXCR4, plasmids for HIV-1 Env panels (subtypes A, B, B′, C, G, A/C, A/E, and B/C), and molecular clones of HIV reference strains (HIV-1_{NL4-3} and HIV-2_{ROD}) were obtained through the AIDS Reagent Program, Division of AIDS, NIAID, NIH. Two plasmids encoding SIV Env (pSIVpbj-Env and

pSIV239) were kindly provided by Jianqing Xu at the Shanghai Public Health Clinical Center & Institutes of Biomedical Sciences, Fudan University, China. Cells were cultured in complete growth medium that consisted of Dulbecco's minimal essential medium (DMEM) supplemented with 10% fetal bovine serum, 100 U/ml of penicillin-streptomycin, 2 mM L-glutamine, 1 mM sodium pyruvate, and 1× MEM nonessential amino acids (Gibco/Invitrogen, USA) and were maintained at 37°C in 5% CO_2.

Peptide synthesis. A total of 29 CHR- or NHR-derived peptides were synthesized using a standard solid-phase 9-flurorenylmethoxycarbonyl (FMOC) method as described previously (39). All peptides were acetylated at the N terminus and amidated at the C terminus. Peptide concentrations were determined using UV absorbance and a theoretically calculated molar extinction coefficient, ε, at 280 nm of 5,500 and 1,490 mol/liter per cm based on the number of tryptophan and tyrosine residues, respectively (53).

Single-cycle infection assay. A single-cycle infection assay was performed as described previously (48). Briefly, HIV-1 or SIV pseudoviruses were generated via cotransfection of HEK293T cells with an Env-expressing plasmid and a backbone plasmid, pSG3Δenv, that encodes Env-defective, luciferase-expressing HIV-1 genome. Culture supernatants were harvested 48 h after transfection, and 50% tissue culture infectious doses ($TCID_{50}$) were determined in TZM-bl cells. To measure the antiviral activity of inhibitors, peptides were prepared in 3-fold dilutions, mixed with 100 $TCID_{50}$ of viruses, and then incubated for 1 h at room temperature. The mixture was added to TZM-bl cells (10^4/well) and incubated for 48 h at 37°C. Luciferase activity was measured using luciferase assay reagents and a luminescence counter (Promega, Madison, WI). The percent inhibition of viral entry by the peptides and 50% inhibitory concentration (IC_{50}) values were calculated using GraphPad Prism software (GraphPad Software Inc., San Diego, CA).

Cell-cell fusion assay. A dual split protein (DSP)-based assay was performed to determine HIV or SIV Env-mediated cell-cell fusion as described previously (54, 55). Briefly, a total of 1.5×10^4 293T cells (effector cells) were seeded on a 96-well plate, and a total of 8×10^4 U87-CXCR4 cells (target cells) were seeded on a 24-well plate. On the following day, effector cells were transfected with a mixture of an Env-expressing plasmid and a DSP_{1-7} plasmid, and target cells were transfected with a DSP_{8-11} plasmid. Forty-eight hours posttransfection, the target cells were resuspended in 300 μl prewarmed culture medium, and to each well 0.05 μl EnduRen live cell substrate (Promega) was added. Aliquots of 75 μl of the target cell suspension then were transferred over each well of the effector cells in the presence or absence of serially 3-fold-diluted peptide fusion inhibitors. The cells were then spun down to maximize cell-cell contact and incubated for 1 h at 37°C. Luciferase activity was measured by a luminescence counter (Promega).

Inhibition of infectious HIV-1_{NL4-3} and HIV-2_{ROD} isolates. The anti-HIV activity of peptide inhibitors was initially assessed by using molecular clones of wild-type HIV-1_{NL4-3} and HIV-2_{ROD} as two indicator viruses. Briefly, viral stocks were prepared by transfecting a plasmid (pNL4-3 or pROD) into HEK293T cells. Culture supernatants were harvested 48 h posttransfection and quantified for $TCID_{50}$ in TZM-bl cells. Viruses were used at 100 $TCID_{50}$ to infect TZM-bl cells in the presence or absence of serially 3-fold-diluted peptides. Cells were harvested 2 days postinfection and lysed in reporter lysis buffer, and luciferase activity was measured as described above.

Inhibition of HIV-2 primary isolates. A total of 9 HIV-2 primary isolates were obtained from Portuguese patients by cocultivation with peripheral blood mononuclear cells (PBMCs) from seronegative subjects (14, 24). The antiviral activity of fusion inhibitor peptides was evaluated in TZM-bl cells. First, 10,000 TZM-bl cells were seeded in 96-well tissue culture plates and incubated overnight. The next day, the growth medium was removed and replaced by 200 μl of fresh growth medium supplemented with 19.7 μg/ml of DEAE-dextran. Cells were infected with 200 $TCID_{50}$ of each virus in the presence of 3-fold dilutions of peptides. After 48 h of infection, luciferase expression was quantified with the Pierce firefly luciferase glow assay kit (Thermo Fisher, USA) according to the manufacturer's instructions. The cytotoxicity of the compounds was evaluated using control wells in the absence of the virus. At least two independent experiments were performed for each analysis, and each assay was set up in duplicate wells. The 50% (IC_{50}) and 90% (IC_{90}) inhibitory concentrations, as well as the dose-response curve slopes (Hill slope), were estimated by plotting the percent inhibition of infection (*y* axis) against the $\log_{10}$ concentration of each fusion inhibitor (*x* axis) and using the sigmoidal dose-response (variable slope) equation in GraphPad Prism software.

Inhibition of HIV-2_{ROD} mutants. A panel of HIV-2_{ROD} mutants carrying mutations in amino acid positions of the envelope V3 loop that determine CCR5 and/or CXCR4 usage was used for evaluating the inhibitory activity of the peptides as described above. These mutants were generated in the pROD10 plasmid using the QuikChange II XL site-directed mutagenesis kit (Stratagene) as described previously (45). Mutant viruses were obtained by transient transfection of HEK293T cells using the jetPrime transfection reagent (Polyplus) according to the manufacturer's instructions. Transfections were performed with 10 μg of DNA in a 100-mm tissue culture dish. Cell culture supernatants were collected 48 h posttransfection, filtered, and stored at −80°C until use.

CD spectroscopy. Circular dichroism (CD) spectroscopy was performed according to our previously described protocols (39). Briefly, a CHR peptide was incubated with an equal molar concentration of the NHR peptide N36 at 37°C for 30 min in PBS (pH 7.2). CD spectra were acquired on a Jasco spectropolarimeter (model J-815) using a 1-nm bandwidth with a 1-nm step resolution from 195 to 270 nm at room temperature. Spectra were corrected by subtraction of a solvent blank. The α-helical content was calculated from the CD signal by dividing the mean residue ellipticity (θ) at 222 nm by the value expected for 100% helix formation ($-33{,}000$ degree · cm^2 · dmol^{-1}). Thermal denaturation was performed by monitoring the ellipticity change at 222 nm from 20°C to 98°C at a rate of 2°C/min, and T_m (melting temperature) was defined as the midpoint of the thermal unfolding transition.

ACKNOWLEDGMENTS

We thank Jianqing Xu at the Shanghai Public Health Clinical Center & Institutes of Biomedical Sciences of Fudan University for providing the plasmids encoding SIV Env.

This work was supported by grants from the National Natural Science Foundation of China (81271830, 81473255, 81630061, and 81673484) and from the Fundação para a Ciência e a Tecnologia (FCT), Portugal (PTDC/SAU-EPI/122400/2010 and VIH/SAU/0029/2011). P.B. was supported by a postdoctoral grant from the Fundação para a Ciência e a Tecnologia (FCT), Portugal (SFRH/BPD/112348/2015), and A.M. was supported by a Ph.D. studentship from the Fundação para a Ciência e a Tecnologia, Portugal (SFRH/BD/71028/2010).

REFERENCES

1. UNAIDS. 2015. AIDS by the numbers 2015. UNAIDS, Geneva, Switzerland. http://www.unaids.org/sites/default/files/media_asset/AIDS_by_the_numbers_2015_en.pdf.
2. Valadas E, Franca L, Sousa S, Antunes F. 2009. 20 Years of HIV-2 infection in Portugal: trends and changes in epidemiology. Clin Infect Dis 48:1166–1167. https://doi.org/10.1086/597504.
3. Barin F, Cazein F, Lot F, Pillonel J, Brunet S, Thierry D, Damond F, Brun-Vezinet F, Desenclos JC, Semaille C. 2007. Prevalence of HIV-2 and HIV-1 group O infections among new HIV diagnoses in France: 2003-2006. AIDS 21:2351–2353. https://doi.org/10.1097/QAD.0b013e3282f15637.
4. Guyader M, Emerman M, Sonigo P, Clavel F, Montagnier L, Alizon M. 1987. Genome organization and transactivation of the human immunodeficiency virus type 2. Nature 326:662–669. https://doi.org/10.1038/326662a0.
5. Clavel F, Mansinho K, Chamaret S, Guetard D, Favier V, Nina J, Santos-Ferreira MO, Champalimaud JL, Montagnier L. 1987. Human immunodeficiency virus type 2 infection associated with AIDS in West Africa. N Engl J Med 316:1180–1185. https://doi.org/10.1056/NEJM198705073161903.
6. Ayouba A, Akoua-Koffi C, Calvignac-Spencer S, Esteban A, Locatelli S, Li H, Li Y, Hahn BH, Delaporte E, Leendertz FH, Peeters M. 2013. Evidence for continuing cross-species transmission of SIVsmm to humans: characterization of a new HIV-2 lineage in rural Cote d'Ivoire. AIDS 27:2488–2491. https://doi.org/10.1097/01.aids.0000432443.22684.50.
7. de Silva TI, Cotten M, Rowland-Jones SL. 2008. HIV-2: the forgotten AIDS virus. Trends Microbiol 16:588–595. https://doi.org/10.1016/j.tim.2008.09.003.
8. Damond F, Worobey M, Campa P, Farfara I, Colin G, Matheron S, Brun-Vezinet F, Robertson DL, Simon F. 2004. Identification of a highly divergent HIV type 2 and proposal for a change in HIV type 2 classification. AIDS Res Hum Retrovir 20:666–672. https://doi.org/10.1089/0889222041217392.
9. Lemey P, Pybus OG, Wang B, Saksena NK, Salemi M, Vandamme AM. 2003. Tracing the origin and history of the HIV-2 epidemic. Proc Natl Acad Sci U S A 100:6588–6592. https://doi.org/10.1073/pnas.0936469100.
10. Hu DJ, Dondero TJ, Rayfield MA, George JR, Schochetman G, Jaffe HW, Luo CC, Kalish ML, Weniger BG, Pau CP, Schable CA, Curran JW. 1996. The emerging genetic diversity of HIV. The importance of global surveillance for diagnostics, research, and prevention. JAMA 275:210–216.
11. Ntemgwa ML, d'Aquin Toni T, Brenner BG, Camacho RJ, Wainberg MA. 2009. Antiretroviral drug resistance in human immunodeficiency virus type 2. Antimicrob Agents Chemother 53:3611–3619. https://doi.org/10.1128/AAC.00154-09.
12. Witvrouw M, Pannecouque C, Switzer WM, Folks TM, De Clercq E, Heneine W. 2004. Susceptibility of HIV-2, SIV and SHIV to various anti-HIV-1 compounds: implications for treatment and postexposure prophylaxis. Antiviral Ther 9:57–65.
13. Hizi A, Tal R, Shaharabany M, Currens MJ, Boyd MR, Hughes SH, McMahon JB. 1993. Specific inhibition of the reverse transcriptase of human immunodeficiency virus type 1 and the chimeric enzymes of human immunodeficiency virus type 1 and type 2 by nonnucleoside inhibitors. Antimicrob Agents Chemother 37:1037–1042. https://doi.org/10.1128/AAC.37.5.1037.
14. Borrego P, Calado R, Marcelino JM, Bartolo I, Rocha C, Cavaco-Silva P, Doroana M, Antunes F, Maltez F, Caixas U, Barroso H, Taveira N. 2012. Baseline susceptibility of primary HIV-2 to entry inhibitors. Antiviral Ther 17:565–570. https://doi.org/10.3851/IMP1996.
15. Wild CT, Shugars DC, Greenwell TK, McDanal CB, Matthews TJ. 1994. Peptides corresponding to a predictive alpha-helical domain of human immunodeficiency virus type 1 gp41 are potent inhibitors of virus infection. Proc Natl Acad Sci U S A 91:9770–9774. https://doi.org/10.1073/pnas.91.21.9770.
16. Lalezari JP, Henry K, O'Hearn M, Montaner JS, Piliero PJ, Trottier B, Walmsley S, Cohen C, Kuritzkes DR, Eron JJ, Jr, Chung J, DeMasi R, Donatacci L, Drobnes C, Delehanty J, Salgo M, TORO 1 Study Group. 2003. Enfuvirtide, an HIV-1 fusion inhibitor, for drug-resistant HIV infection in North and South America. N Engl J Med 348:2175–2185. https://doi.org/10.1056/NEJMoa035026.
17. Kilby JM, Hopkins S, Venetta TM, DiMassimo B, Cloud GA, Lee JY, Alldredge L, Hunter E, Lambert D, Bolognesi D, Matthews T, Johnson MR, Nowak MA, Shaw GM, Saag MS. 1998. Potent suppression of HIV-1 replication in humans by T-20, a peptide inhibitor of gp41-mediated virus entry. Nat Med 4:1302–1307. https://doi.org/10.1038/3293.
18. Chan DC, Kim PS. 1998. HIV entry and its inhibition. Cell 93:681–684. https://doi.org/10.1016/S0092-8674(00)81430-0.
19. Weissenhorn W, Dessen A, Harrison SC, Skehel JJ, Wiley DC. 1997. Atomic structure of the ectodomain from HIV-1 gp41. Nature 387:426–430. https://doi.org/10.1038/387426a0.
20. Tan K, Liu J, Wang J, Shen S, Lu M. 1997. Atomic structure of a thermostable subdomain of HIV-1 gp41. Proc Natl Acad Sci U S A 94:12303–12308. https://doi.org/10.1073/pnas.94.23.12303.
21. Chan DC, Fass D, Berger JM, Kim PS. 1997. Core structure of gp41 from the HIV envelope glycoprotein. Cell 89:263–273. https://doi.org/10.1016/S0092-8674(00)80205-6.
22. Rimsky LT, Shugars DC, Matthews TJ. 1998. Determinants of human immunodeficiency virus type 1 resistance to gp41-derived inhibitory peptides. J Virol 72:986–993.
23. Greenberg ML, Cammack N. 2004. Resistance to enfuvirtide, the first HIV fusion inhibitor. J Antimicrob Chemother 54:333–340. https://doi.org/10.1093/jac/dkh330.
24. Borrego P, Calado R, Marcelino JM, Pereira P, Quintas A, Barroso H, Taveira N. 2013. An ancestral HIV-2/simian immunodeficiency virus peptide with potent HIV-1 and HIV-2 fusion inhibitor activity. AIDS 27:1081–1090. https://doi.org/10.1097/QAD.0b013e32835edc1d.
25. Menendez-Arias L, Alvarez M. 2014. Antiretroviral therapy and drug resistance in human immunodeficiency virus type 2 infection. Antiviral Res 102:70–86. https://doi.org/10.1016/j.antiviral.2013.12.001.
26. He Y. 2013. Synthesized peptide inhibitors of HIV-1 gp41-dependent membrane fusion. Curr Pharm Des 19:1800–1809. https://doi.org/10.2174/1381612811319100004.
27. Berkhout B, Eggink D, Sanders RW. 2012. Is there a future for antiviral fusion inhibitors? Curr Opin Virol 2:50–59. https://doi.org/10.1016/j.coviro.2012.01.002.
28. Steffen I, Pohlmann S. 2010. Peptide-based inhibitors of the HIV envelope protein and other class I viral fusion proteins. Curr Pharm Des 16:1143–1158. https://doi.org/10.2174/138161210790963751.
29. Eggink D, Berkhout B, Sanders RW. 2010. Inhibition of HIV-1 by fusion inhibitors. Curr Pharm Des 16:3716–3728. https://doi.org/10.2174/138161210794079218.
30. Martin-Carbonero L. 2004. Discontinuation of the clinical development of fusion inhibitor T-1249. AIDS Rev 6:61.
31. Eron JJ, Gulick RM, Bartlett JA, Merigan T, Arduino R, Kilby JM, Yangco B,

Diers A, Drobnes C, DeMasi R, Greenberg M, Melby T, Raskino C, Rusnak P, Zhang Y, Spence R, Miralles GD. 2004. Short-term safety and antiretroviral activity of T-1249, a second-generation fusion inhibitor of HIV. J Infect Dis 189:1075–1083. https://doi.org/10.1086/381707.
32. Dwyer JJ, Wilson KL, Davison DK, Freel SA, Seedorff JE, Wring SA, Tvermoes NA, Matthews TJ, Greenberg ML, Delmedico MK. 2007. Design of helical, oligomeric HIV-1 fusion inhibitor peptides with potent activity against enfuvirtide-resistant virus. Proc Natl Acad Sci U S A 104:12772–12777. https://doi.org/10.1073/pnas.0701478104.
33. He Y, Xiao Y, Song H, Liang Q, Ju D, Chen X, Lu H, Jing W, Jiang S, Zhang L. 2008. Design and evaluation of sifuvirtide, a novel HIV-1 fusion inhibitor. J Biol Chem 283:11126–11134. https://doi.org/10.1074/jbc.M800200200.
34. Gustchina E, Hummer G, Bewley CA, Clore GM. 2005. Differential inhibition of HIV-1 and SIV envelope-mediated cell fusion by C34 peptides derived from the C-terminal heptad repeat of gp41 from diverse strains of HIV-1, HIV-2, and SIV. J Med Chem 48:3036–3044.
35. Chong H, Yao X, Qiu Z, Sun J, Qiao Y, Zhang M, Wang M, Cui S, He Y. 2014. The M-T hook structure increases the potency of HIV-1 fusion inhibitor sifuvirtide and overcomes drug resistance. J Antimicrob Chemother 69:6759.
36. Chong H, Qiu Z, Sun J, Qiao Y, Li X, He Y. 2014. Two M-T hook residues greatly improve the antiviral activity and resistance profile of the HIV-1 fusion inhibitor SC29EK. Retrovirology 11:40. https://doi.org/10.1186/1742-4690-11-40.
37. Chong H, Yao X, Qiu Z, Sun J, Zhang M, Waltersperger S, Wang M, Liu SL, Cui S, He Y. 2013. Short-peptide fusion inhibitors with high potency against wild-type and enfuvirtide-resistant HIV-1. FASEB J 27:1203–1213. https://doi.org/10.1096/fj.12-222547.
38. Chong H, Yao X, Sun J, Qiu Z, Zhang M, Waltersperger S, Wang M, Cui S, He Y. 2012. The M-T hook structure is critical for design of HIV-1 fusion inhibitors. J Biol Chem 287:34558–34568. https://doi.org/10.1074/jbc.M112.390393.
39. Chong H, Yao X, Qiu Z, Qin B, Han R, Waltersperger S, Wang M, Cui S, He Y. 2012. Discovery of critical residues for viral entry and inhibition through structural insight of HIV-1 fusion inhibitor CP621-652. J Biol Chem 287:20281–20289. https://doi.org/10.1074/jbc.M112.354126.
40. Chong H, Wu X, Su Y, He Y. 2016. Development of potent and long-acting HIV-1 fusion inhibitors. AIDS 30:1187–1196. https://doi.org/10.1097/QAD.0000000000001073.
41. Chong H, Qiu Z, Su Y, Yang L, He Y. 2015. Design of a highly potent HIV-1 fusion inhibitor targeting the gp41 pocket. AIDS 29:13–21. https://doi.org/10.1097/QAD.0000000000000498.
42. deCamp A, Hraber P, Bailer RT, Seaman MS, Ochsenbauer C, Kappes J, Gottardo R, Edlefsen P, Self S, Tang H, Greene K, Gao H, Daniell X, Sarzotti-Kelsoe M, Gorny MK, Zolla-Pazner S, LaBranche CC, Mascola JR, Korber BT, Montefiori DC. 2014. Global panel of HIV-1 Env reference strains for standardized assessments of vaccine-elicited neutralizing antibodies. J Virol 88:2489–2507. https://doi.org/10.1128/JVI.02853-13.
43. Su Y, Chong H, Xiong S, Qiao Y, Qiu Z, He Y. 2015. Genetic pathway of HIV-1 resistance to novel fusion inhibitors targeting the gp41 pocket. J Virol 89:12467–12479. https://doi.org/10.1128/JVI.01741-15.
44. Su Y, Chong H, Qiu Z, Xiong S, He Y. 2015. Mechanism of HIV-1 resistance to short-peptide fusion inhibitors targeting the gp41 pocket. J Virol 89:5801–5811. https://doi.org/10.1128/JVI.00373-15.
45. Martins A, Calado M, Borrego P, Marcelino J, Azevedo-Pereira J. 2016. Determinants of coreceptor use, tropism and susceptibility to antibody neutralization in the V3 region of HIV-2. Keystone Symposia conference X7: HIV persistence: pathogenesis and eradication. Keystone Symposia, Silverthorne, CO.
46. Colman PM, Lawrence MC. 2003. The structural biology of type I viral membrane fusion. Nat Rev Mol Cell Biol 4:309–319. https://doi.org/10.1038/nrm1076.
47. Eckert DM, Kim PS. 2001. Mechanisms of viral membrane fusion and its inhibition. Annu Rev Biochem 70:777–810. https://doi.org/10.1146/annurev.biochem.70.1.777.
48. Yao X, Chong H, Zhang C, Waltersperger S, Wang M, Cui S, He Y. 2012. Broad antiviral activity and crystal structure of HIV-1 fusion inhibitor sifuvirtide. J Biol Chem 287:6788–6796. https://doi.org/10.1074/jbc.M111.317883.
49. Liu Z, Shan M, Li L, Lu L, Meng S, Chen C, He Y, Jiang S, Zhang L. 2011. In vitro selection and characterization of HIV-1 variants with increased resistance to sifuvirtide, a novel HIV-1 fusion inhibitor. J Biol Chem 286:3277–3287. https://doi.org/10.1074/jbc.M110.199323.
50. Caffrey M, Cai M, Kaufman J, Stahl SJ, Wingfield PT, Covell DG, Gronenborn AM, Clore GM. 1998. Three-dimensional solution structure of the 44 kDa ectodomain of SIV gp41. EMBO J 17:4572–4584. https://doi.org/10.1093/emboj/17.16.4572.
51. Malashkevich VN, Chan DC, Chutkowski CT, Kim PS. 1998. Crystal structure of the simian immunodeficiency virus (SIV) gp41 core: conserved helical interactions underlie the broad inhibitory activity of gp41 peptides. Proc Natl Acad Sci U S A 95:9134–9139. https://doi.org/10.1073/pnas.95.16.9134.
52. Chan DC, Chutkowski CT, Kim PS. 1998. Evidence that a prominent cavity in the coiled coil of HIV type 1 gp41 is an attractive drug target. Proc Natl Acad Sci U S A 95:15613–15617. https://doi.org/10.1073/pnas.95.26.15613.
53. Gill SC, von Hippel PH. 1989. Calculation of protein extinction coefficients from amino acid sequence data. Anal Biochem 182:319–326. https://doi.org/10.1016/0003-2697(89)90602-7.
54. Ishikawa H, Meng F, Kondo N, Iwamoto A, Matsuda Z. 2012. Generation of a dual-functional split-reporter protein for monitoring membrane fusion using self-associating split GFP. Protein Eng Des Sel 25:813–820. https://doi.org/10.1093/protein/gzs051.
55. Kondo N, Miyauchi K, Meng F, Iwamoto A, Matsuda Z. 2010. Conformational changes of the HIV-1 envelope protein during membrane fusion are inhibited by the replacement of its membrane-spanning domain. J Biol Chem 285:14681–14688. https://doi.org/10.1074/jbc.M109.067090.